*J. exp. Biol.* **149**, 449–468 (1990)
*Printed in Great Britain* © *The Company of Biologists Limited 1990*



# BODY DRAG, FEATHER DRAG AND INTERFERENCE DRAG OF THE MOUNTING STRUT IN A PEREGRINE FALCON, *FALCO PEREGRINUS*

BY VANCE A. TUCKER
*Department of Zoology, Duke University, Durham, NC 27706, USA*

*Accepted 31 October 1989*

## Summary

1. The mean, minimum drag coefficients ($C_{D,B}$) of a frozen, wingless peregrine falcon body and a smooth-surfaced model of the body were 0.24 and 0.14, respectively, at air speeds between 10.0 and 14.5 $m\,s^{-1}$. These values were measured with a drag balance in a wind tunnel, and use the maximum cross-sectional area of the body as a reference area. The difference between the values indicates the effect of the feathers on body drag. Both values for $C_{D,B}$ are lower than those predicted from most other studies of avian body drag, which yield estimates of $C_{D,B}$ up to 0.41.

2. Several factors must be controlled to measure minimum drag on a frozen body. These include the condition of the feathers, the angle of the head and tail relative to the direction of air flow, and the interference drag generated by the drag balance and the strut on which the body is mounted.

3. This study describes techniques for measuring the interference drag generated by (a) the drag balance and mounting strut together and (b) the mounting strut alone. Corrections for interference drag may reduce the apparent body drag by more than 20 %.

4. A gliding Harris' hawk (*Parabuteo unicinctus*), which has a body similar to that of the falcon in size and proportions, has an estimated body drag coefficient of 0.18. This value can be used to compute the profile drag coefficients of Harris' hawk wings when combined with data for this species in the adjoining paper (Tucker and Heine, 1990).

## Introduction

A complete analysis of avian aerodynamics divides a flying bird into its various parts and describes the aerodynamic forces on them. The first step in the analysis conventionally separates the wings from the rest of the bird – the 'body' in this study. The drag component of the aerodynamic force on a bird's body is known as 'body drag' or sometimes 'parasite drag' because it is not associated with a significant lift component.

Key words: bird flight, drag coefficient, gliding performance, Harris' hawk, parasite drag, polar curve, wind tunnel.

Recent studies of gliding flight (Tucker, 1987, 1988; Tucker and Heine, 1990) use body drag as one of the terms in a mathematical model that calculates the aerodynamic forces on a bird's wings and predicts the bird's gliding performance. These studies estimate body drag from an equation (Tucker, 1973) fitted to drag measurements on seven frozen, wingless bird bodies mounted on drag balances in wind tunnels. More recent studies of body drag (Prior, 1984; Pennycuick *et al.* 1988) report variable results and raise questions about interference drag on bodies mounted on drag balances and the effect of the feathers on the drag of frozen bodies.

This study reports drag measurements in a wind tunnel on the frozen, wingless body of a peregrine falcon and on an accurate, smooth-surfaced model of that body. It has two purposes: (1) to remedy technical problems in measuring body drag, and (2) to obtain an accurate estimate of the body drag of a Harris' hawk (*Parabuteo unicinctus*, a bird of the same size as the falcon), whose gliding performance is described in an adjoining paper (Tucker and Heine, 1990).

## Theory

Air moving past an object creates an aerodynamic force with components that are perpendicular and parallel to the flow direction. The perpendicular component (lift) is negligible in this study, but drag (the parallel component) varies with the size and shape of the object and with the speed, density and viscosity of the air. 'Shape' includes the orientation of the object relative to the air flow and its surface roughness. Air viscosity and density are constant in this study. I shall describe drag with two related quantities that are less dependent on size and speed: the equivalent flat plate area and the drag coefficient. More information on these quantities may be found in standard aerodynamic textbooks such as von Mises (1959), in an adjoining paper in this journal (Tucker and Heine, 1990) and in Vogel (1981) and Pennycuick (1989).

### *Equivalent flat plate area*

The equivalent flat plate area ($S_{fp}$) is the ratio of the drag ($D$) on an object to the theoretical pressure on a flat plate (see following description of pressure drag) held perpendicular to the air flow:

$$S_{fp} = D/(0.5\rho V^2), \quad (1)$$

where $V$ is air speed and $\rho$ is air density. $S_{fp}$ is useful for calculating the drag on an object of a given size at different air speeds because it varies with size but relatively little with speed.

### *Drag coefficients and Reynolds number*

The drag coefficient ($C_D$) is the ratio of drag on an object to the theoretical aerodynamic force on a flat plate of area $S$ held perpendicular to the air flow:

$$C_D = D/(0.5\rho S V^2). \quad (2)$$

$S$ is a reference area on the object, chosen to make $C_D$ relatively independent of both size of the object and air speed. Thus, $C_D$ is useful for calculating the drag of objects of different sizes and air speeds. $C_D$ is related to $S_{fp}$ since

$$C_D = S_{fp}/S. \tag{3}$$

Drag coefficients may vary with Reynolds number ($Re$):

$$Re = \rho d V/\mu, \tag{4}$$

where $d$ is a reference length of the object and $\mu$ is the viscosity of the air. The ratio $\rho/\mu$ (the reciprocal of kinematic viscosity) has the value 68 436 s m$^{-2}$ for air at sea level in the US standard atmosphere (von Mises, 1959).

I use two different definitions of reference area and reference length for bird bodies (exclusive of the wings) in this study. The cross-sectional area ($S_B$) is the maximum area of the body in a plane perpendicular to the direction of air flow when the body is oriented to have minimum drag ($D_B$) and drag coefficient ($C_{D,B}$) at a given speed – i.e. when the long axis of the body is approximately parallel to the direction of air flow. [Tucker and Heine (1990) discussed the parasite drag of an intact bird and used the symbol $D_{par,B}$ for $D_B$.] The corresponding reference length ($d_B$) is the diameter of a circle of area $S_B$ (Prior, 1984; Pennycuick *et al.* 1988):

$$d_B = 2(S_B/\pi)^{0.5}. \tag{5}$$

The wetted area ($S_w$) is the total surface area of the body – i.e. the area that would be wetted if the body were dipped in water. The corresponding reference length ($d_w$) is the total length of the body from the tip of the beak to tip of the tail.

*Reynolds number based on body mass and speed*

For bird bodies, any one of these quantities can be calculated from the other two. Pennycuick *et al.* (1988) described $S_B$ for raptors and waterfowl as a function of body mass ($m$):

$$S_B = 0.00813 m^{0.666}. \tag{6}$$

Substituting equation 6 into equation 5, and equation 5 into equation 4 yields

$$Re = 2\rho(0.00813/\pi)^{1/2} m^{0.333} V/\mu, \tag{7}$$

or, for the standard atmosphere at sea level,

$$Re = 6963 m^{0.333} V. \tag{8}$$

*Skin friction, pressure drag and separation*

Body drag is the sum of skin friction drag and pressure drag. The following discussion summarizes relevant information from Goldstein (1965) and von Mises (1959).

An infinitely thin flat plate held parallel to the air flow illustrates pure skin friction drag. The air in contact with the plate sticks to the surface and, because air

is viscous, this stationary layer influences the speed of the air in a boundary layer next to the plate. The air flow in the boundary layer may be either laminar or turbulent. Air in a laminar boundary layer flows in essentially the same direction as the air immediately outside the boundary layer. Air in a turbulent boundary layer flows in different directions.

Skin friction drag for a laminar boundary layer on a parallel plate is less than that for a turbulent boundary layer. Drag coefficients based on wetted area are given by the formula of Blasius for a laminar boundary layer:

$$C_{f,lam} = 1.328Re^{-0.5}, \tag{9}$$

and the formula of Prandtl for a turbulent boundary layer:

$$C_{f,tur} = 0.455(\log_{10}Re)^{-2.58} \tag{10}$$

The reference length for $Re$ is the length of the plate parallel to the flow direction. For example, the ratio $C_{f,lam}/C_{f,tur}$ is 0.40 at a typical $Re$ value of 380 000 (based on $d_w$) for the falcon body in this study.

Pure pressure drag arises on an idealized, infinitely thin flat plate held perpendicular to the flow direction. The pressure in the undisturbed flow, and in the theoretical wake behind the plate, is $P$. At the edges of the plate, air flow separates between the free stream flow and the wake. Air flow comes to a stop at the upstream face of the plate and exerts pressure $P+0.5\rho V^2$. The difference in pressure between the upstream face of the plate and the relatively low pressure wake is $0.5\rho V^2$, and the drag on the plate is $0.5\rho V^2 S$. $S$ is the area of the upstream face of the plate, and the drag coefficient for the reference area $S$ has a value of 1.

The condition of the boundary layer on a three-dimensional object influences the tendency of the air flow to separate from the object and, thereby, influences pressure drag. When the boundary layer is turbulent, air tends to cling to rounded eminences and flow around them rather than separating and leaving a low-pressure wake. The opposite is true of a laminar boundary layer. In contrast to skin friction drag, a turbulent boundary layer reduces pressure drag and a laminar boundary layer increases it. Whether the boundary layer on an object is laminar or turbulent depends on the shape of the object, its Reynolds number and the turbulence of the air before it flows over the object.

The drag coefficients of rounded objects may decrease sharply when the boundary layer in certain regions goes through the transition from laminar to turbulent. For example, the drag coefficient of a sphere with a laminar boundary layer at the point of separation may drop by half when the speed, and hence the Reynolds number, increases by 20%. The increase in $Re$ causes the boundary layer to become turbulent, and the air flows further around the sphere before separating. The smaller wake reduces pressure drag.

Many birds fly at Reynolds numbers where rounded objects have significant areas of both laminar and turbulent boundary layers. The bird's body surface can be seen as a mosaic of patches, some with separated air flow and others with laminar or turbulent boundary layers. The patches are in a delicate balance

seemingly minor changes in the turbulence and speed of the air, and in the shape of the bird's body, may change their sizes and locations. As a result, both skin friction and pressure drag may change markedly with the minor changes mentioned.

### *Interference drag*

The body drag of a bird is usually measured on a wingless body mounted on the strut of a drag balance in a wind tunnel. The balance measures both drag on the body and drag on the strut, and current practice is to compute the drag on the isolated body by subtracting the drag of the isolated strut – i.e. the drag of the strut with nothing mounted on it. However, this procedure does not entirely correct for the effects of the strut because the air flow around the body mounted on the strut differs from that around the isolated parts and generates additional drag known as 'interference drag'. The measured drag ($D_m$) is the sum of the drags on the isolated body ($D_B$) and the isolated strut ($D_s$) plus the interference drag ($D_I$):

$$D_m = D_B + D_s + D_I . \tag{11}$$

In the present study, the mounting strut extended from a streamlined shroud that shielded the drag balance and part of the strut from the wind and reduced strut drag. Both the strut and the shroud influence the air flow around the bird body and cause interference drag. I shall first describe how the position of the shroud influences both the isolated strut drag and the interference drag, and then describe a method for measuring interference drag.

#### *Shroud position*

A shroud may be designed to cover all of the strut, in which case it extends to the bird body, or it may be lower and leave some of the strut exposed. If a shroud that extends to the body is lowered progressively at a particular air speed, the measured drag first decreases to a minimum and then increases (Fig. 1), for reasons explained below.

Interference drag ($D_I$) is the sum of the interference drag due to the strut ($D_{I,s}$) and the interference drag due to the shroud ($D_{I,sh}$):

$$D_I = D_{I,s} + D_{I,sh} . \tag{12}$$

As the shroud is lowered, $D_I$ decreases because the decrease in $D_{I,sh}$ from the large shroud is greater than the increase in $D_{I,s}$ from the small strut. However, the strut drag increases as the lowered shroud exposes more strut length ($d_s$). Measured drag reaches a minimum (Fig. 1) when the decrease in $D_{I,sh}$ equals the increase in strut drag. Measured drag then increases because strut drag increases, $D_{I,s}$ remains the same and $D_{I,sh}$ approaches zero.

A quantitative model for the relationship between measured drag and the exposed length of the strut is:

$$D_m = D_B + rd_s + D_{I,s} + D_{I,sh} , \tag{13}$$

where $r$ is a constant equal to the rate of change of strut drag with length. The

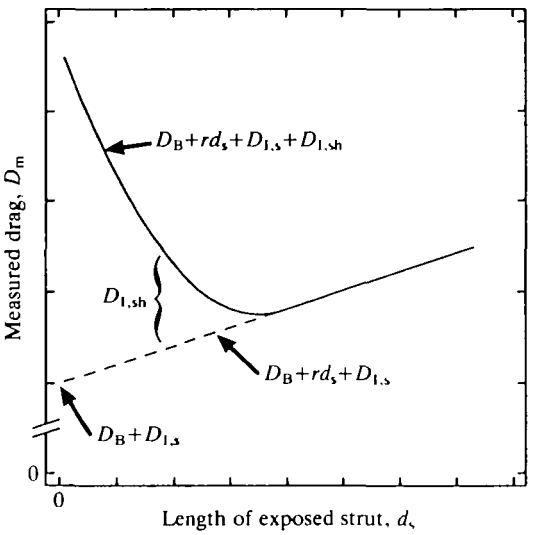


Fig. 1. Influence of shroud position, expressed as the length ($d_s$) of the exposed strut, on measured drag ($D_m$) at a constant air speed. The dashed line is an extrapolation. See text and equation 13 for explanation.

ascending part of the curve in Fig. 1, along which $D_{I,sh}$ is negligible, extrapolates to the intercept $D_m=D_B+D_{I,s}$ when $d_s=0$. This intercept also equals $D_{m,0}-D_{s,0}$, where $D_{m,0}$ is the measured drag at a particular strut length ($d_s$,0) at which $D_{I,sh}$ is negligible. The strut drag at $d_{s,0}$ is $D_{s,0}$.

The shroud position on the flight balance in this study made $D_{I,sh}$ negligible. To simplify nomenclature, the following discussion ascribes all of $D_I$ to $D_{I,s}$.

*Measuring interference drag*

The conventional method for determining interference drag uses combinations of multiple mounting struts (Gorlin and Slezinger, 1966; Pope and Harper, 1966). I used a new method in this study based on changing the drag of a single strut and extrapolating to zero. At a given speed, the drag of the isolated strut ($D_s$) can be made large or small by changing the cross-sectional shape of the strut. As $D_s$ approaches zero, the interference drag also approaches zero; and the measured drag ($D_m$) of a body mounted on the strut approaches $D_B$ (Fig. 2). Although there is a mechanical limit to how small $D_s$ can be, the curve relating it to $D_m$ extrapolates to $D_m=D_B$ at $D_s=0$.

When $D_m$ and $D_s$ are linearly related (as they are in this study, see Fig. 5) at a given speed ($V_0$):

$$D_m = k_1 D_s + k_2 . \tag{14}$$

Five useful quantities can be calculated with this equation.

(1) *Body drag at speed* $V_0$. At $D_s=0$,

$$D_B = D_m = k_2 . \tag{15}$$

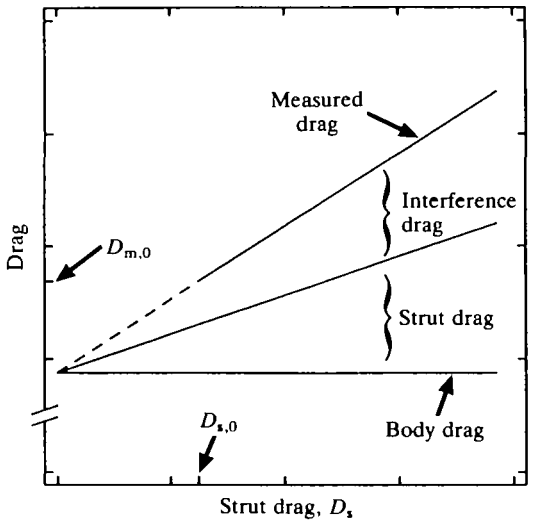


Fig. 2. Influence of strut drag ($D_s$) at constant air speed on measured drag and interference drag for a body mounted on a strut with various cross-sectional shapes. Measured drag is the sum of body drag, strut drag and interference drag. The curve for measured drag extrapolates (dashed line) to body drag. $D_{m,0}$ is the measured drag of a body mounted on the particular strut with the lowest drag ($D_{s,0}$).

(2) *Body drag at other speeds.* The sum $D_s+D_I$ at speed $V_0$ may be expressed as an equivalent flat plate area and subtracted from an equivalent flat plate area for $D_m$ to determine the equivalent flat plate area of the body ($S_{fp,B}$). Body drag and $C_{D,B}$ can then be calculated for other speeds.

Let $D_{s,0}$ and $D_{I,0}$ be the strut drag and interference drag, respectively, of a particular strut at speed $V_0$. $D_{m,0}$ is the drag measured by the flight balance. Substituting equation 15 into equation 11 and rearranging:

$$D_{s,0} + D_{I,0} = D_{m,0} - k_2 . \tag{16}$$

The equivalent flat plate area ($S_{fp,s+I}$) of the strut and interference drag is:

$$S_{fp,s+I} = (D_{m,0} - k_2)/(0.5\rho V_0^2) . \tag{17}$$

Assuming that $S_{fp,s+I}$ is constant over a range of speeds, it follows from equation 11 that

$$S_{fp,B} = D_m/(0.5\rho V^2) - S_{fp,s+I} . \tag{18}$$

(3) *Interference drag as a proportion of strut drag.* Substituting for $D_m$ in equation 11 from equation 14, and for $D_B$ from equation 15:

$$D_I = (k_1 - 1)D_s . \tag{19}$$

(4) *Strut drag as a proportion* ($k_3$) *of measured drag*. By solving equation 14 for $D_s$ and dividing by $D_m$:

$$D_s/D_m = (1 - k_2/D_m)/k_1 = k_3 . \quad (20)$$

(5) *Correction factor for body drag when* $D_I$ *is ignored*. The difference $D_m - D_s$ that has been used to calculate the body drag of birds gives an erroneous value ($D_{B,e}$) because it ignores $D_I$. The correction factor ($F_I$) remedies this error:

$$D_B = F_I D_{B,e} . \quad (21)$$

The correction factor depends only on the slope ($k_1$) of the $D_m$ *vs* $D_s$ curve (equation 14) and the strut drag as a proportion ($k_3$) of measured drag (equation 20). Since $D_B = k_2$ and $k_2 = D_m - k_1 D_s$ (equation 14):

$$\begin{aligned} D_B/D_{B,e} &= (D_m - k_1 D_s)/(D_m - D_s) \\ &= (1 - k_1 D_s/D_m)/(1 - D_s/D_m) . \end{aligned} \quad (22)$$

Substituting $k_3$ for $D_s/D_m$ (equation 20):

$$D_B/D_{B,e} = (1 - k_1 k_3)/(1 - k_3) = F_I . \quad (23)$$

Authors sometimes report $k_3$ as well as $D_{B,e}$, and equation 23 helps to estimate the error factor in such cases.

## Materials and methods

### *Wind tunnel and drag balance*

I measured the drag of a frozen falcon body and a model body mounted on a drag balance in a wind tunnel (described in Tucker and Parrott, 1970; and Tucker and Heine, 1990). The tunnel was set to air speeds equivalent to 10.0, 12.4 and 14.5 $m\,s^{-1}$ at sea level in the US standard atmosphere (air density=1.23 $kg\,m^{-3}$, von Mises, 1959). When making measurements on the frozen body, I varied the speeds in alternating sequences of ascending and descending order.

The drag balance was a parallelogram type, similar to that shown in Fig. 6.65 of Gorlin and Slezinger (1966). A digital voltmeter measured the imbalance of four strain gauges connected in a bridge circuit and attached to the flexible beams of the parallelogram. I calibrated the balance by hanging a weight from a thread that attached to the bird body (or the strut, for measurements on an isolated strut) after running over a pulley on a ball-bearing. The ball-bearing (New Hampshire Bearing SR168) was specially constructed to have low starting torque, and it transferred the gravitational force on the weight to the balance with a change of less than 0.7 %. The accuracy of this measurement system is shown in Table 1.

The drag balance was inside the wind tunnel, shielded from the wind by a wing-shaped, streamlined shroud with a maximum aerofoil thickness of 2.5 cm where the mounting strut extended from the shroud. The chord of the shroud was 3.8 cm at this point and increased to a maximum of 24.3 cm at a level 13 cm lower. The maximum aerofoil thickness where the shroud covered the drag balance was

Table 1. *Accuracy of measurements*

| Quantity | Relative bias (%) | Relative imprecision (%) |
|---|---|---|
| Air speed | 0.035 | 0.23 |
| Drag | 0.070 | 3.3 |
| Digitized points | 0.25 | 0.25 |

Bias is the difference between the mean value ($M$) of repeated measurements of a quantity and the true mean, and imprecision is the standard deviation of repeated measurements of a quantity (Eisenhart, 1968). Relative bias and imprecision are expressed as percentages of the maximum values of $M$ used in this study.

3.9 cm. The trailing edge of the shroud tapered from blunt where the chord was minimum to sharp where the chord was maximum.

The mounting strut had a streamlined cross-section with a maximum thickness of 3.2 mm and a chord of 12.7 mm. It was exposed to the air flow for 9 cm between the top of the shroud and the body mounted on it.

### *Frozen body*

The US Fish and Wildlife Service provided the body of a peregrine falcon that in life had a mass of 0.713 kg. The wings had been cut off at mid-humerus to leave the proximal humeral feathers attached to the body. These feathers smoothly covered the stump of the humerus (which was folded back parallel to the body surface) and the region where each wing had been removed.

To mount the body on the strut of the drag balance, I froze a cylindrical wooden plug into a hole drilled in the ventral midline of the frozen body. The plug was 15.9 mm in diameter, fitted flush with the skin and contained a threaded aluminium insert. A rod attached to the end of the strut screwed into the insert.

I trimmed the body for minimum drag by measuring its drag, then thawed the body just enough to make the neck and tail movable. I preened the feathers with tweezers and refroze the body on its back on a board after propping the head and tail in the desired positions with loose rolls of gauze tape. I measured body drag again and repeated the process to attain minimum drag. During all measurements, the sunken eyeballs were restored to lifelike contours with modelling clay, the feet were tucked up under the tail, and the angle of the entire body on the mounting strut was adjusted for minimum drag.

I was unable to preen the feathers to lie in the smooth, orderly, overlapping pattern that they assumed in a living Harris' hawk in flight (Tucker and Heine, 1990). The feathers on a newly frozen body have gaps between them and flat spots where the body pressed down on them. Some feather shafts are misaligned and the barbs on the shafts tend to separate. By preening the body when it was slightly thawed rather than entirely thawed or frozen, I was able to remove the flat spots

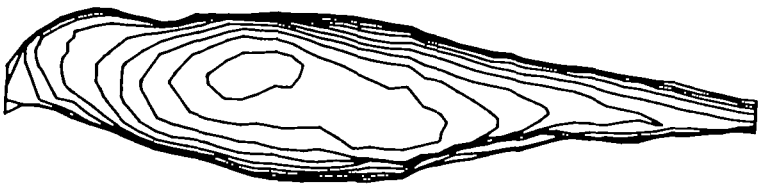

Fig. 3. Contour map of the falcon body, excluding the beak and the terminal 8 cm of the tail. Contour interval=5.77 mm. The part of the body shown in the drawing is 0.357 m long.

and most of the gaps in the feathers and improve the alignment of the feather shafts. The result was a body that looked smooth and unruffled.

*Model body*

The model was a light-weight casting of a plaster body sculpted around two armatures of laminated plywood. The armatures represented the feathered surfaces of the right and left halves of the frozen falcon body in its minimum drag configuration.

To construct the armatures, I measured 999 three-dimensional coordinates on one side of the frozen body with a digitizer (accuracy shown in Table 1). The digitizer arm ended in a needle point that could be placed anywhere in a horizontal plane. I mounted the body vertically in an apparatus that could be raised or lowered with a rack and pinion gear. I recorded coordinates of points around a cross-section at the base of the beak by touching the needle point to the feather surface at the dorsal midline and then moving the needle in steps to the ventral midline along the feather surface of half the circumference. Then I raised the body 7.93 mm with the rack and pinion and digitized the feather surface of the next (more posterior) half-circumference. The needle moved in up to 30 steps per half-circumference, with smaller steps where the radius of curvature was small. The last half-circumference was 8 cm from the tip of the tail. A computer used the complete set of coordinates as data for a program that plotted a life-size contour map of one side of the body (Fig. 3).

The contour interval (5.77 mm) on the map equalled the thickness of the plywood laminations plus the glued joint between them. For each contour line, I glued a copy of the map to two pieces of plywood held together with screws. I then sawed along the contour lines to form identical pairs of plywood laminations, one for each side of the body. I stacked the pairs in register and drilled two index holes through the entire stack. I then peeled the map from each pair, removed the screws, arranged the laminations for each side of the body in order, aligned them on dowels through the index holes, glued them together and completed the sculpture by filling the steps between laminations with plaster and sanding the plaster smooth.

I made plaster-of-Paris moulds of both sculptures and cast them in orthopaedic foam (Pedilen rigid foam, Otto Bock, Duderstadt, Germany). I glued the casts

together after partially hollowing out their insides and attached balsa-wood carvings of the beak and tail feathers. The resulting model body had a mass of 0.2 kg and a surface with the texture of sanded plaster that duplicated the linear dimensions of the frozen body within 2 %.

### *Interference drag*

I investigated the interference drag on the model body due to the shroud (see Theory) at a wind speed of 12.4 m $s^{-1}$ by measuring drag with the shroud at different heights from 23 mm to 14.6 cm below the body.

I determined interference drag on the frozen body due to the strut (see Theory) at a wind speed of 12.4 m $s^{-1}$ by using three struts: the unmodified strut and two modifications of it that increased its drag in steps. The modifications were strips of wood along both its sides and parallel to its long axis. The smaller strips had a circular cross-section with a diameter of 2.2 mm, and the larger strips had a half-round cross-section with a diameter of 12.7 mm. I then measured the drag ($D_m$) of the body mounted on the various struts, and the drag ($D_s$) of the struts alone.

## Results

### *Interference drag*

The relationship between the position of the shroud on the drag balance and the measured drag conformed to the description in the Theory section and to equation 13. The interference drag due to the shroud ($D_{I,sh}$) in this study is negligible, since the point that describes the normal strut length (9 cm) and the measured drag of the model mounted on the strut falls on the ascending part of the curve that relates $D_m$ to $d_s$ (Fig. 4). This part of the curve extrapolates to an intercept of $D_{m,0}-D_{s,0}$ at $d_s=0$, as expected.

Interference drag due to the shroud became negligible when the exposed strut length was three times the aerofoil thickness of the shroud. This factor is specific for the combination of drag balance and falcon body used in the present study, but it can serve as a starting point for evaluating the interference drag of other bodies and drag balances.

The measured drag ($D_m$) of the frozen body mounted on the different struts varied linearly with strut drag (Fig. 5), as in equation 14 (repeated here):

$$D_m = k_1 D_s + k_2 ,$$

with $k_1=1.62$ and $k_2=0.1439$ N ($N=8$, standard deviation around line=0.00327 N). The drag ($D_{s,0}$) of the isolated, unmodified strut was 0.00825 N ($N=4$, standard deviation=0.00570 N).

The values of $k_1$, $k_2$ and $D_{s,0}$ may be used with equations 14–23 to calculate other quantities related to interference drag. For example, the measured drag ($D_{m,0}$) for $D_{s,0}$ is 0.1573 N (equation 14), the strut drag is 5.2 % of measured drag (equation 20), the interference drag is 62.2 % of strut drag (equation 19) and the

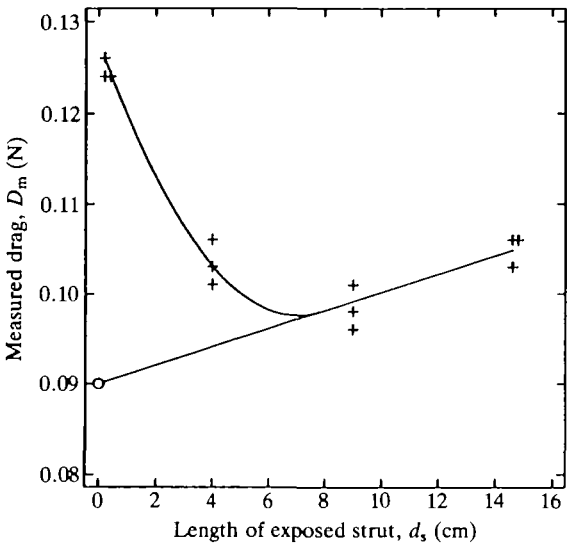


Fig. 4. Influence of shroud position, measured as the exposed strut length ($d_s$), on the measured drag ($D_m$) of the falcon model at a speed of 12.4 m s$^{-1}$. The point marked with a circle for $D_m$ at $d_s$=0 is the mean value of $D_{m,0}-D_{s,0}$. $D_{m,0}$ and $D_{s,0}$ are the measured drags on the model and the isolated strut, respectively, for the normal configuration of the drag balance (strut length=9 cm). Identical points are shown slightly offset.

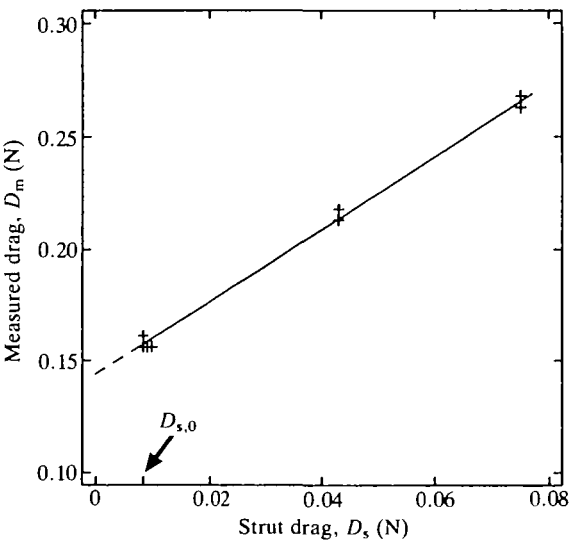


Fig. 5. Influence of strut drag ($D_s$) on the measured drag ($D_m$) of the frozen falcon body at a speed of 12.4 m s$^{-1}$. $D_{s,0}$ is the drag of the unmodified strut. Identical points are shown slightly offset.

Table 2. *Dimensions of the frozen body and the model*

| Dimension | Symbol | Value |
|---|---|---|
| Maximum cross-sectional area | $S_B$ | $0.00669\,m^2$ |
| Wetted area | $S_w$ | $0.844\,m^2$ |
| Total length | $d_w$ | $0.447\,m^2$ |

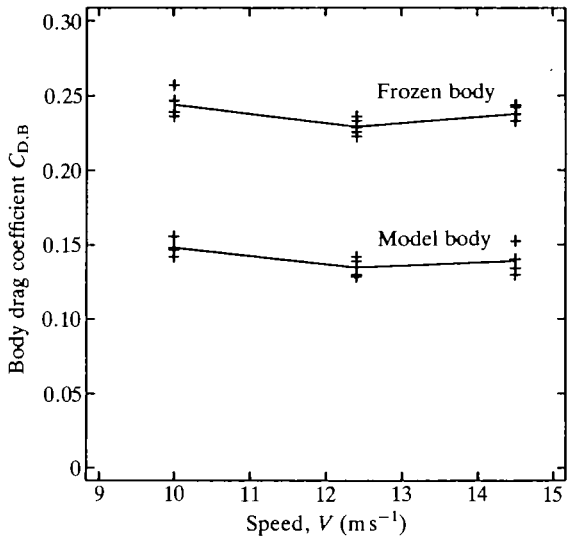


Fig. 6. The drag coefficients of the frozen falcon body (top curve) and the model body (bottom curve).

equivalent flat plate area of strut drag plus interference drag is $0.000142\,m^2$ (equation 17). I used this value for both the frozen body and the model.

### *Dimensions of the frozen body and the model*

I computed dimensions (Table 2) from the three-dimensional coordinates of the model, plus measurements on the balsa-wood beak and tail. These dimensions also describe the frozen body.

### *Drag coefficients of the frozen body and the model*

Drag coefficients of both the frozen body and the model varied in the same way with speed, but the values for the model were only about 60 % of those for the frozen body (Fig. 6 and Table 3). Analysis of variance indicates that the differences between the mean $C_{D,B}$ values at different speeds are highly significant.

Table 3. *Drag coefficients of the frozen body and the model*

| | Frozen body | | Model | |
|---|---|---|---|---|
| Speed ($m s^{-1}$) | Mean $C_{D,B}$ | S.D. ($N$) | Mean $C_{D,B}$ | S.D. ($N$) |
| 10.0 | 0.244 | 0.007668 (6) | 0.148 | 0.005590 (4) |
| 12.4 | 0.229 | 0.004888 (6) | 0.135 | 0.006607 (4) |
| 14.5 | 0.238 | 0.004380 (6) | 0.139 | 0.009716 (4) |

## Discussion

The literature contains a wide range of values for the drag coefficients of wingless bird bodies (see Fig. 8). Some of the variation can be explained by differences among species but, where large variation is seen even between similar species, uncontrolled factors in the measurement process may be responsible. The results of the present study implicate shape factors – the smoothness of the feathers and the trim of the body – and the interference drag of the mounting system.

### *Shape factors*

#### *Condition of the feathers*

The feathered surface caused a large proportion of the drag on the falcon body in this study, since the drag of the model was only about 60 % of that of the frozen body (Table 2). The rougher surface of the feathered body compared with the model probably increased drag by thickening the boundary layer, and influenced the distribution of the laminar and turbulent boundary layers and separated flow. Feathers that flutter in the wind probably have high pressure drag, as do fluttering flags (Hoerner, 1965). The effects of the compliance and porosity of the feathered surface on drag are unknown.

Pennycuick *et al.* (1988) also noticed an effect of feathers on drag. The feathers on some bird bodies fluffed out as speed increased, and body drag did not return to its original value when speed decreased. The authors were able to reduce by 15 % the drag on a snow goose body by smoothing down the feathers and holding them in place with hair spray. In the present study, the feathers on the falcon body did not appear to fluff out, and the drag measurements were not affected by the direction of speed change.

#### *Body trim*

'Trim' refers to the angles between head, torso and tail and the air flow. I could change the drag on the falcon body by 25 % by adjusting these angles through a range of lifelike configurations.

### *Interference drag*

Interference drag can be significant if the drag of the isolated mounting strut (o

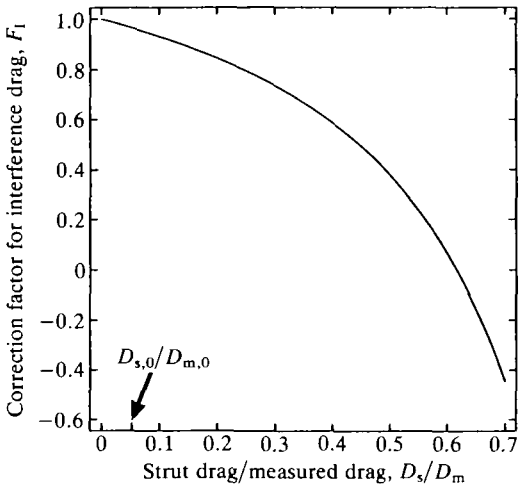


Fig. 7. The relationship between strut drag ($D_s$) as a proportion of measured drag ($D_m$) and the correction factor for interference drag. The correction factor multiplied by the difference between measured drag and strut drag gives body drag. The curve shows equation 23 when $k_1=1.62$, a value specific for the frozen falcon body mounted on the balance used in the present study at a speed of $12.4\,m\,s^{-1}$. The ratio $D_{s,0}/D_{m,0}$ describes the unmodified mounting strut used in the present study.

struts) is a large proportion of the measured drag. For example, when the strut drag is 25 % of the measured drag, the body drag is only 79 % (Fig. 7) of the value usually reported as body drag (the difference between measured drag and strut drag). The curve in the figure is specific for the falcon body and mounting system used in this study, but it indicates the magnitude of the errors that can arise in other systems.

### *Comparisons with other measurements*

The body drag coefficients reported by various authors for wingless, frozen bodies of several bird species can be related to Reynolds number (Fig. 8). The figure also shows the measured drag coefficients of the falcon model and the drag coefficients the model would have if its drag were the same as that on a parallel plate of the same wetted area with a turbulent boundary layer (equation 10). I shall describe these data in more detail below and review the information provided by the authors on (1) how they smoothed the feathers, trimmed the body, and corrected for interference drag and (2) the accuracy (Eisenhart, 1968) of the measurement process.

#### *Data from Pennycuick (1968, 1971)*

Pennycuick measured the drag coefficients (circles at top left of Fig. 8) of a pigeon (1968) and an African vulture (1971). The pigeon was frozen with its head raised above the position that is typical for free flight. The vulture was frozen in a position judged typical for free flight with minimum drag.

*Data from Tucker (1973)*

These data (crosses at the top left of Fig. 8) come from equivalent flat plate areas for a budgerigar, sparrow, starling, falcon and a mallard. I converted them to drag coefficients by dividing by cross-sectional body areas from equation 6. My

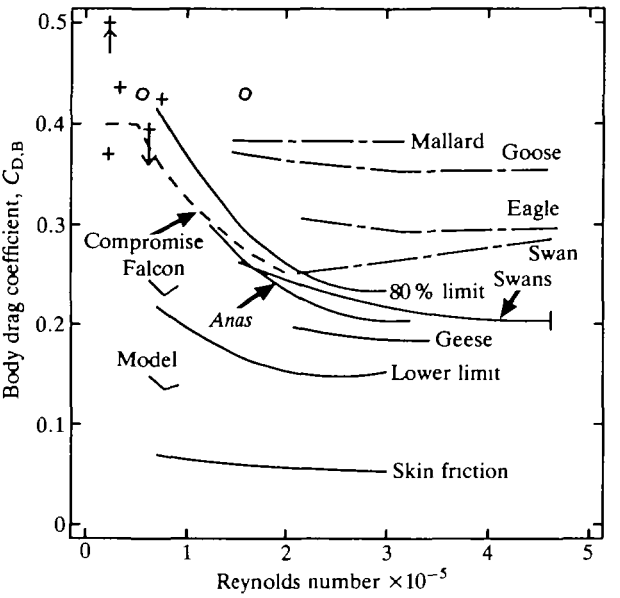


Fig. 8. Drag coefficients ($C_{D,B}$) of bird bodies at different Reynolds numbers. Points marked + at upper left are from Tucker (1973). The upward-pointing arrow indicates an off-scale point for a sparrow ($C_{D,B}$=0.56), and the downward-pointing arrow connects $C_{D,B}$ for a laggar falcon to a value corrected for interference drag (arrow point). Points marked with circles at upper left are from Pennycuick (1968, 1971). Broken curves at upper right and dashed 'compromise' curve are from Pennycuick *et al.* (1988). Skin friction curve is from equation 10, assuming body drag of the falcon model is entirely due to skin friction drag from a turbulent boundary layer. Other solid curves are from Prior (1984) (equations for curves are given in Table 4; curve for swans is truncated by bar) and from the present study. The Reynolds number for a bird of a given mass at a given speed at sea level can be estimated from equation 8.

Table 4. *Summary equations for Prior's $C_{D,B}$ data*

| Description | $C_{D,B}$ | Range of $x$* |
|---|---|---|
| 80% limit† | $0.553-0.224x+0.0391x^2$ | 0.7–3.0 |
| Lower limit† | $0.282-0.106x+0.0211x^2$ | 0.7–3.0 |
| Genus *Anas*‡ | $0.474-0.177x+0.0291x^2$ | 1.2–3.2 |
| Geese‡ | $0.286-0.063x+0.0096x^2$ | 2.1–3.4 |
| Swans‡ | $0.345-0.065x+0.0074x^2$ | 1.5–5.2 |

*$x$=Reynolds number$\times 10^{-5}$.
†Curves fitted by Pennycuick *et al.* (1988).
‡Curves fitted in present study.

1973 paper described the bodies as arranged in 'natural flight attitudes' but did not say whether they were trimmed for minimum drag (I did not systematically adjust the body parts) or how the feathers were preened (I smoothed them on the frozen bodies). The paper specified the accuracy of the measurement process.

I can estimate the interference drag on the 1973 falcon (a 0.571-kg laggar falcon, *Falco jugger*, similar to the peregrine falcon in the present study) from the original data. The drag of the mounting strut was 12 % of the measured drag, and correcting for its interference drag reduces $C_{D,B}$ from 0.40 to 0.36. The latter value in Fig. 8 is at the tip of the arrow that extends downwards from the uncorrected value.

*Data from Prior (1984)*

Prior (1984) measured the drag on 30 frozen bodies of 17 species of water fowl ranging in size from small ducks to swans. Pennycuick *et al.* (1988) summarized Prior's data with two curves (Fig. 8): one fitted to the lower boundary of the data and the other fitted above about 80 % of the data. (The excluded data are markedly above the rest of Prior's results.) I have fitted curves (Fig. 8) to Prior's data for ducks, geese and swans for comparison with other body drag measurements on these groups.

Prior rotated the bodies in the wind tunnel to obtain minimum drag. He assumed that streamlined mounting struts caused negligible interference drag.

*Data from Pennycuick* et al. *(1988)*

These authors measured body drag for a mallard, an eagle, a goose and a swan (curves at top right of Fig. 8) after smoothing the feathers on the frozen bodies. Although they did not correct for interference drag, they noted that the drag of the support system amounted to about 40 % of the total drag for the larger bodies, and that the support bar apparently caused the feathers in its wake to flutter. They expressed reservations about the accuracy of their measurements because the drag balance operated near the lower limit of its range where they could not determine the linearity or repeatability of its readings. Their drag coefficients were higher than those of Prior, and they suggested a compromise curve (dashed in Fig. 8) to describe drag coefficients as a function of Reynolds number.

One can use Fig. 7 to estimate the error introduced by interference drag in the results of Pennycuick *et al.* (1988). For the body and mounting system used in the present study, the corrected drag coefficient is 59 % of the uncorrected drag when the strut drag is 40 % of the measured drag. However, these authors used a different mounting system with various bodies, and one might plausibly assume that the interference drag of their system was equivalent to that of the system in the present study when the strut drag equals 25 % of measured drag. Then, corrected drag coefficients would be 79 % of those shown in Fig. 8.

*Data from the present study*

The measurements made in this study yield a much lower estimate of the drag

coefficient for a falcon than my 1973 measurements. I attribute this reduction to careful preening of the feathers on the partially thawed body, adjusting the body parts for minimum drag, and reducing interference drag and correcting for it.

### *Streamlining, skin friction and pressure drag*

Objects may be classified as streamlined or unstreamlined, depending on whether skin friction drag or pressure drag predominates. The drag of streamlined objects may be only 10% more than the skin friction drag on a parallel plate of equivalent wetted area when the boundary layers on both objects are turbulent (Goldstein, 1965). Unstreamlined objects may have much greater pressure drag than skin friction drag. For example, a sphere with a laminar boundary layer up to the region of separation has a large pressure drag because of its large wake. The drag on the sphere may be 30 times the drag on a parallel plate of equivalent wetted area with a laminar boundary layer (Goldstein, 1965).

Bird bodies are relatively unstreamlined (Prior, 1984; Pennycuick *et al.* 1988). All the drag coefficients in Fig. 8 are more than twice what they would be if body drag were equal only to the skin friction drag on a parallel plate of equal wetted area with a turbulent boundary layer. Indeed, the pressure drags on bird bodies are even greater than comparisons with the curve for coefficients based on skin friction indicate. Birds fly at Reynolds numbers where significant areas of both laminar and turbulent boundary layers exist on rounded objects (Goldstein, 1965), and skin friction drag is less for a laminar than for a turbulent boundary layer.

The drag on bird bodies may be quite sensitive to changes in Reynolds number, surface roughness and air turbulence because transition from a laminar to a turbulent boundary layer can cause a large change in pressure drag (see Theory).

### *Drag coefficient of the Harris' hawk body*

The preceding discussion shows that any estimate of a body drag coefficient for the Harris' hawk based on body mass or Reynolds number will be controversial. Instead, I shall use the measurements on the falcon body and model in the present study. The intact falcon had nearly the same mass (0.713 kg) as the hawk (0.702 kg), and their bodies had similar proportions. Although the drag coefficients for the falcon and the model are lower than those reported by others, the present study controlled factors that can generate high drag coefficients.

The drag coefficients for the Harris' hawk are probably somewhere between those for the frozen falcon body and those for the model. The surface of the Harris' hawk in flight was smooth, more like that of the model. However, the model did not accurately reproduce all the surface details of the frozen body – for example, the contours where the cere merged with the beak, the groove between the eyeball and the brow, and the individual toes of the retracted feet. Considering these factors, I shall use a drag coefficient of 0.18, the mean of the drag coefficients of the frozen body and the model at 12.4 $m\,s^{-1}$, for a Harris' hawk gliding at its

normal range of flight speeds. The corresponding equivalent flat plate area is $0.00120\,m^2$.

I am grateful to Mark Fuller, US Fish and Wildlife Service, for providing the falcon body, and to Carlton Heine for building the flight balance.

**List of symbols**

| | |
|---|---|
| $C_D$ | drag coefficient |
| $C_{D,B}$ | body drag coefficient |
| $C_{f,lam}$ | skin friction coefficient, laminar boundary layer |
| $C_{f,tur}$ | skin friction coefficient, turbulent boundary layer |
| $D$ | drag on an object |
| $D_B$ | body drag |
| $D_{B,e}$ | erroneous body drag |
| $D_I$ | interference drag |
| $D_{I,0}$ | interference drag of a particular strut |
| $D_{I,s}$ | interference drag of strut |
| $D_{I,sh}$ | interference drag of shroud |
| $D_m$ | measured drag of a body on a strut |
| $D_{m,0}$ | measured drag of a body on a particular strut |
| $D_s$ | strut drag |
| $D_{s,0}$ | drag of a particular strut |
| $d$ | reference length for Reynolds number |
| $d_B$ | diameter of circle with area $S_B$ |
| $d_s$ | exposed length of strut |
| $d_{s,0}$ | exposed length of a particular strut |
| $d_w$ | length of body from beak to tail |
| $F_I$ | correction factor for interference drag |
| $k_1$, $k_2$ | slope and intercept, respectively, of equation 14 |
| $k_3$ | ratio of strut drag to measured drag |
| $M$ | mean value of repeated measurements |
| $m$ | body mass |
| $N$ | sample size |
| $P$ | air pressure |
| $Re$ | Reynolds number |
| $r$ | rate of change of strut drag with strut length |
| $S$ | reference area |
| $S_B$ | maximum cross-sectional area of a bird body |
| $S_{fp}$ | equivalent flat plate area |
| $S_{fp,B}$ | equivalent flat plate area of body |
| $S_{fp,s+I}$ | equivalent flat plate area of strut drag plus interference drag |
| $S_w$ | wetted area |
| $V$ | air speed |
| $V_0$ | a specified air speed |
| $\mu$ | viscosity of air |

$\pi$ ratio of circumference to diameter of a circle
$\rho$ air density

## References

EISENHART, C. (1968). Expression of uncertainties in final results. *Science* **160**, 1201–1204.
GOLDSTEIN, S. (1965). *Modern Developments in Fluid Dynamics*, vol. II. New York: Dover Publications.
GORLIN, S. M. AND SLEZINGER, I. I. (1966). *Wind Tunnels and Their Intrumentation*. Jerusalem, Israel: Israel Program for Scientific Translations.
HOERNER, S. F. (1965). *Fluid-dynamic Drag*. Brick Town, NJ: S. F. Hoerner.
PENNYCUICK, C. J. (1968). A wind-tunnel study of gliding flight in the pigeon *Columba livia*. *J. exp. Biol.* **49**, 509–526.
PENNYCUICK, C. J. (1971). Control of gliding angle in a Rüppell's griffon vulture *Gyps rüppellii*. *J. exp. Biol.* **55**, 39–46.
PENNYCUICK, C. J. (1989). *Bird Flight Performance: a Practical Calculation Manual*. Oxford: Oxford University Press.
PENNYCUICK, C. J., OBRECHT, H. H. AND FULLER, M. R. (1988). Empirical estimates of body drag of large waterfowl and raptors. *J. exp. Biol.* **135**, 253–264.
POPE, A. AND HARPER, J. J. (1966). *Lowspeed Wind Tunnel Testing*. New York: Wiley & Sons.
PRIOR, N. C. (1984). Flight energetics and migration performance of swans. PhD dissertation, University of Bristol.
TUCKER, V. A. (1973). Bird metabolism during flight: evaluation of a theory. *J. exp. Biol.* **58**, 689–709.
TUCKER, V. A. (1987). Gliding birds: the effect of variable wing span. *J. exp. Biol.* **133**, 33–58.
TUCKER, V. A. (1988). Gliding birds: descending flight of the white-backed vulture, *Gyps africanus*. *J. exp. Biol.* **140**, 325–344.
TUCKER, V. A. AND HEINE, C. (1990). Aerodynamics of gliding flight in the Harris' hawk, *Parabuteo unicinctus*. *J. exp. Biol.* **149**, 469–489.
TUCKER, V. A. AND PARROTT, C. G. (1970). Aerodynamics of gliding flight in a falcon and other birds. *J. exp. Biol.* **52**, 345–367.
VOGEL, S. (1981). *Life in Moving Fluids*. Princeton: Princeton University Press.
VON MISES, R. (1959). *Theory of Flight*. New York: Dover Publications.